



Title	Enrichment of chlorophyll catabolic enzymes in grana margins and their cooperation in catabolic reactions
Author(s)	Fukura, Koki; Tanaka, Ayumi; Tanaka, Ryouichi; Ito, Hisashi
Citation	Journal of plant physiology, 266, 153535 https://doi.org/10.1016/j.jplph.2021.153535
Issue Date	2021-11-01
Doc URL	http://hdl.handle.net/2115/90640
Rights	©2021. This manuscript version is made available under the CC-BY-NC-ND 4.0 license http://creativecommons.org/licenses/by-nc-nd/4.0/
Rights(URL)	http://creativecommons.org/licenses/by-nc-nd/4.0/
Type	article (author version)
File Information	Journal of plant physiology_266_153535.pdf



[Instructions for use](#)

Title

Enrichment of chlorophyll catabolic enzymes in grana margins and their cooperation in catabolic reactions

Authors

Koki Fukura^{1,2}, Ayumi Tanaka², Ryouichi Tanaka², Hisashi Ito²

¹Graduate School of Life Science, Hokkaido University, N10 W8, Sapporo 060-0810, Japan, ²Institute of Low Temperature Science, Hokkaido University, N19 W8, Sapporo 060-0819, Japan

Abbreviations

CBB, Coomassie brilliant blue; CBR, chlorophyll *b* reductase; GDN, glyco-diosgenin; Chl, chlorophyll; HCAR, 7-hydroxymethyl chlorophyll *a* reductase; HMChl *a*, 7-hydroxymethyl chlorophyll *a*; HPLC, high-performance liquid chromatography; LHCII, light-harvesting complex of photosystem II; NOL, non-yellow coloring 1-like; NYC1, non-yellow coloring 1; PAO, pheophorbide *a* oxygenase; PS, photosystem; SGR, Stay-Green; SGRL, SGR-like; WT, wild-type

Abstract

During leaf senescence, chlorophyll *a* and *b* are degraded through several enzymatic reactions, including chlorophyll *b* reductase, 7-hydroxymethyl chlorophyll *a* reductase, and Mg-dechelatase. Considering that the intermediates of the chlorophyll breakdown pathway are highly photoreactive, cooperative and efficient reactions of chlorophyll metabolic enzymes may protect chloroplasts from potential photo-oxidative damage. Here, we investigated the sub-organellar localization and cooperative reactions of the enzymes involved in the chlorophyll breakdown pathway by the fractionation of thylakoid membranes and enzymatic assays using recombinant proteins. We found that these enzymes were enriched in the grana margin fraction. Furthermore, we found that chlorophyll *b* reductase and Mg-dechelatase efficiently catabolized chlorophylls bound to the chlorophyll–protein complexes when these two enzymes were mixed. These results suggest that the co-localization of chlorophyll catabolic enzymes enables efficient chlorophyll breakdown. The results from this study highlight a key step forward in the investigation of the photosystem breakdown process.

Keywords

Arabidopsis, chlorophyll breakdown, chlorophyll *b* reductase, Mg-dechelatase, thylakoid fractionation, grana margin

Introduction

Chlorophyll (Chl) breakdown is a remarkable feature of leaf senescence (Kuai et al., 2018). The first step in Chl *a* breakdown is the extraction of the central Mg by Mg-dechelatase to form pheophytin *a*. This enzyme is also called Stay-Green (SGR; also known as NYE1) because the gene encoding this enzyme has been identified in mutant plants that show a stay-green phenotype at the senescent stage. Most angiosperms have several isoforms of Mg-dechelatase, all of which share sequence similarities. One isoform of SGR, which is constitutively expressed in the leaves, is called SGR-like (SGRL). The phytol group of pheophytin *a* is removed to form pheophorbide *a*; the pheophorbide ring is then opened by pheophorbide *a* oxygenase (PAO) for further breakdown.

Neither SGR nor SGRL can react with Chl *b* (Shimoda et al., 2016). Therefore, Chl *b* should be converted to Chl *a* prior to breakdown. The first step in the conversion of Chl *b* to Chl *a* is the reduction of the C-7 formyl group of Chl *b* to a hydroxymethyl group by Chl *b* reductase (CBR) to produce 7-hydroxymethyl chlorophyll *a* (HMChl *a*). CBR has two isoforms, known as non-yellow coloring 1 (NYC1) and NYC1-like (NOL). NYC1 is expressed at the senescence stage, whereas NOL is constitutively expressed. HMChl *a* is then reduced to Chl *a* by 7-hydroxymethyl chlorophyll *a* reductase (HCAR). The accumulation of Chl breakdown intermediates causes photo-oxidative damage. Therefore,

the reactions of Chl breakdown must be coordinated to minimize the accumulation of the intermediates.

The thylakoid membrane in chloroplasts can be divided into three domains: the grana core, grana margin, and stroma lamellae. While sites of photosystem formation have been investigated (Danielsson et al., 2006; Puthiyaveetil et al., 2014), there are few reports on the degradation of photosystems. The grana margin is supposed to be the site of photosystem degradation (Koochak et al., 2019; Puthiyaveetil et al., 2014). However, it is still not known exactly where Chl breakdown occurs in the thylakoid membrane. If photosystems are degraded at the grana margin, Chl breakdown is also likely to occur there itself.

Functional interaction of catabolic enzymes has been implicated based on observations of mutant plants with defective Chl catabolic enzymes. For example, PAO- and pheophytinase-deficient plants accumulate their substrates—pheophorbide *a* and pheophytin *a*—and also delay Chl breakdown at the senescent stage (Pruzinska et al., 2003; Schelbert et al., 2009). Considering that PAO and pheophytinase do not catabolize Chl, the suppression of Chl breakdown in these mutants suggests the functional interaction of these enzymes and SGR. Functional interaction of the enzymes may be achieved by the co-localization of related enzymes in the thylakoid membrane. To understand the Chl and photosystem breakdown processes, we examined the localization and enzymatic activity of Chl catabolic enzymes.

Materials and methods

Plant growth conditions and transmission electron microscopy

Wild-type (WT) and SGR-deficient mutant *Arabidopsis thaliana* (Col-0) plants were grown under 12 h light/12 h dark conditions at 24 °C for 4 weeks. An SGR-deficient mutant was obtained by crossing mutants lacking SGR1 (Ren et al., 2007) (a kind gift from Prof. B. Kuai, Fudan University), SGR2 (SALK_003830C), and SGRL (SALK_084849), as previously reported (Chen et al., 2021). Senescence was induced by placing the SGR-deficient mutant under dark conditions for 7 days.

Chloroplasts were observed using a transmission electron microscope (H-7650, Hitachi), as previously described (Chen et al., 2021).

Thylakoid sub-fractionation and protein analysis

Thylakoid membrane preparation and sub-fractionation were performed as previously reported (Nishioka et al., 2021). Briefly, isolated thylakoid membranes were suspended in a buffer (50 mM HEPES-KOH, pH 7.5; 100 mM sorbitol; 2 mM MgCl₂; 10 mM NaF) containing 1% v/v protease inhibitor cocktail for plant cell and tissue extracts (Sigma-Aldrich) at 0.6 mg mL⁻¹ Chl concentration. The thylakoid membrane suspension was mixed

with the same volume of 1.6% (w/v) glyco-diosgenin (GDN; anatrace) solubilized in water. After incubation for 10 min at 25 °C, the non-solubilized membranes were removed by centrifugation at 1,000 $\times g$ for 1 min at 4 °C. The supernatant was then centrifuged at 40,000 $\times g$ for 30 min at 4 °C. The pellets were used as the core fraction of grana. The supernatant was further centrifuged at 140,000 $\times g$ for 90 min at 4 °C. The loose pellet and rigid pellet were used as the grana margin fraction and stroma lamellar fraction, respectively. We repeated fractionation experiments at least two times.

For Coomassie brilliant blue (CBB) staining, samples containing 7.5 μg of Chl were applied to polyacrylamide gels. Immunoblotting was performed as previously described (Chen et al., 2021). Briefly, proteins were separated by SDS-PAGE, and the electrophoresed proteins were transferred onto a polyvinylidene difluoride membrane. The primary antibodies were diluted with an immunoreaction enhancer solution (Can Get Signal, Toyobo). Anti-rabbit IgG linked to horseradish peroxidase was used as the secondary antibody. Horseradish peroxidase activity was visualized using a Western Lightning Plus-ECL (PerkinElmer). For the detection of PsaA/B, PsaD, and other Chl proteins, samples containing 0.15, 3.75, and 1.5 μg Chl were applied. For the detection of Chl catabolic enzymes, samples containing 3.75 μg of Chl were applied. For CURT1A detection, samples containing 1.5 μg of Chl were applied. For D1 analysis, the polyacrylamide gel contained 6 M urea. For CURT1A analysis, Tricine-SDS-PAGE optimized for low-molecular-weight protein separation was used (Schägger, 2006). PsaA/B was detected using an antibody against CP1. We purchased antibodies against PsaD (AS09 461), D1 (AS11 1786), Lhca2 (AS01 006), Lhcb4 (AS04 045), CURT1A (AS08 316), and PAO (AS11 1783) proteins from Agrisera. The anti-CP1 (PsaA/PsaB) and anti-CP43 antibodies were prepared as previously described (Tanaka et al., 1991). The anti-NYC1, anti-NOL, and anti-HCAR antibodies against purified recombinant proteins were prepared as previously described (Horie et al., 2009; Meguro et al., 2011). The CP1 primary antibody was diluted to 1:20,000, PsaD, Lhca2, Lhcb4, and PAO primary antibodies were diluted to 1:10,000, D1 and CP43 primary antibodies were diluted to 1:5,000, NYC1, NOL, and HCAR primary antibodies were diluted to 1:3,000, and the CURT1A primary antibody was diluted to 1:1,000.

For the quality analysis of the antibodies, proteins were extracted from leaves and used for immunoblotting, as previously reported (Chen et al., 2021).

Recombinant protein preparation

Arabidopsis NOL (AT5G04900) and Arabidopsis SGRL (AT1G44000) expression plasmids were constructed as previously reported (Horie et al., 2009; Obata et al., 2019). The constructed plasmids were introduced into *Escherichia coli* BL21 (DE3) cells. Recombinant proteins were expressed in an auto-induction medium (6 g Na₂HPO₄, 3 g KH₂PO₄, 20 g tryptone, 5 g yeast extract, 5 g NaCl, 6 mL glycerol, 5 g glucose, 2 g lactose, and 100 mg kanamycin in 1 L) at 37 °C for 16 h with shaking at 120 rpm (Studier, 2005). After the

induction of the recombinant protein, cultured cells (100 mL) were harvested by centrifugation at 7,000 $\times g$ for 5 min. The pellet was resuspended in buffer A (20 mM Na-phosphate, pH 7.4; 100 mM NaCl; 20 mM imidazole) and disrupted by sonication (Branson Sonifier SFX250, Branson: output 8, duty cycle 20%) for 6 min in an ice bath. Supernatant cleared of the cell lysate was obtained by centrifugation at 20,000 $\times g$ for 10 min and then loaded onto a 5 mL HisTrap HP column (Cytiva) equilibrated with buffer A using an ÄKTAprime plus (Cytiva). The recombinant proteins were eluted with buffer B (20 mM Na-phosphate, pH 7.4; 100 mM NaCl; 500 mM imidazole). Protein purity was examined by SDS-PAGE and CBB staining, as reported previously (Chen et al., 2021).

Enzymatic assay of the recombinant protein

The thylakoid membrane fraction (0.6 μg Chl) prepared from WT Arabidopsis was incubated with the recombinant protein (1.2 μg) in 50 μL solution (20 mM Na-phosphate, pH 7.4; 100 mM NaCl; 1 mM NADPH; 0.05% Triton X-100) at 37 °C for 1 h. After incubation, the pigments were analyzed by high-performance liquid chromatography (HPLC), as reported previously (Obata et al., 2019). Pheophytin a was monitored at 680 nm emission and 410 nm excitation with a fluorescence detector (RF-20A; Shimadzu). HMChl a was monitored by measuring the absorbance at 653 nm with a diode array detector (SPD-M10A; Shimadzu).

Results and discussion

Thylakoid membrane fractionation

Among the Chl catabolic enzymes, we examined NYC1, NOL, HCAR, and PAO, for which antibodies are available (Fig. S1). Since NYC1 accumulates only in senescent leaves (Kuai et al., 2018), we needed to prepare the thylakoid membrane from such leaves. Chloroplast membrane structures rapidly and heterogeneously collapse with the progression of leaf senescence, which makes the fractionation of thylakoid membranes by centrifugation difficult. Thus, we used SGR-deficient mutant plants as a source of senescing thylakoids, as these plants retain thylakoid membranes even during senescence (Chen et al., 2021).

The senescence of SGR-deficient mutant plants was induced by placing the plants in the dark for 7 days. Transmission electron microscopy showed that the chloroplasts of senescent SGR-deficient plants maintained their membrane structure (Fig. S2). Thylakoid membranes were isolated from WT and SGR-deficient plants with or without senescence induction under dark conditions. Thylakoid membranes were fractionated into the grana core, grana margin, and stroma lamellae by differential centrifugation. Recently, the use of GDN, which has an analogous structure to digitonin, has been reported for thylakoid membrane fractionation (Nishioka et al., 2021). We used GDN as a substitute for digitonin in this study because it is an artificial and homogenous chemical and a compatible

detergent to solubilize the thylakoid membrane homogeneously. The Chl *a/b* ratio is a marker for evaluating the quality of the isolated thylakoid domains. The Chl *a/b* ratio is reported to be in the order of grana core, grana margin, and stroma lamella (Nishioka et al., 2021). The data from one typical experiment are shown in Table 1. Our results were generally consistent with this order.

Localization of the enzymes involved in Chl breakdown

The purity of the thylakoid membrane fractions was examined by protein staining (Fig. S3) and immunoblotting (Fig. 1) after SDS-PAGE. The light-harvesting complex of PSII (LHCII) and ATPase bands were enriched in the grana core and grana margin fractions, respectively (Fig. S3). These observations are consistent with those of previous reports (Puthiyaveetil et al., 2014). PSI and PSII are abundant in the stroma lamella and grana core, respectively. Our immunoblotting also showed that PSI (PsaA/B, PsaD, Lhca2) was enriched in the stroma lamellar fraction, and PSII (D1, CP43, Lhcb4) was enriched in the grana core fraction (Fig. 1). PSI and PSII are known to be located in the grana margin. The grana margin fraction also contained PSI and PSII. CURT1A was specifically found in the grana margin. Our immunoblotting results showed that CURT1A was enriched in the grana margin fraction. Overall, immunoblotting was consistent with a previous report (Wang et al., 2016). We concluded that we successfully fractionated the thylakoid membrane.

Next, we examined NYC1, NOL, HCAR, and PAO by immunoblotting. NYC1 accumulated in the senescent leaves of the SGR-deficient mutant (Fig. 1). NYC1 was enriched in the grana margin fraction. NOL, HCAR, and PAO were also enriched in the grana margin fraction. Although NOL, HCAR, and PAO are hydrophilic proteins, at least some of them were recovered in the thylakoid membrane fraction. This is reasonable because their substrates occur in the thylakoid membrane. All the enzymes we examined were enriched in the grana margin fraction, suggesting that Chl breakdown occurs in the grana margin. Our observations are consistent with a model in which photosystems are degraded in the grana margin (Koochak et al., 2019; Puthiyaveetil et al., 2014).

Cooperative reactions of CBR and SGR in Chl bound to Chl-protein complexes

The core subunits of photosystems bind only to Chl *a*, whereas LHCII binds both Chl *a* and Chl *b*. It has been suggested that the conversion of Chl *b* to Chl *a* is necessary not only for Chl *b* breakdown but also for Chl *a* breakdown in LHCII. CBR-deficient plants show a delay in both Chl *a* and Chl *b* breakdown (Kusaba et al., 2007), even though the mutant has SGR. Accordingly, this mutant retains LHCII throughout the senescence stage. In contrast, the breakdown of LHCII was also delayed in SGR-deficient plants (Chen et al., 2021), which is deficient in Chl *a* breakdown. It is possible that the cooperative degradation of both Chl *a* and Chl *b* is necessary for the efficient breakdown of these pigments in LHCII.

Previous studies have shown that recombinant SGR and CBR can catabolize Chl *a* and Chl *b* bound to isolated photosynthetic complexes, respectively (Horie et al., 2009; Shimoda et al., 2016). In this study, we investigated the functional cooperation between CBR and SGR. CBR has two homologs, namely, NYC1 and NOL. NOL was used as CBR for the biochemical assay because NOL was successfully expressed in *E. coli*, whereas NYC1 was not because of its transmembrane domain (Kusaba et al., 2007). As described in the Introduction section, Arabidopsis contains three SGR family proteins: SGR1, SGR2, and SGRL. Given the difficulty in expressing SGR1 and SGR2 in *E. coli* (Obata et al., 2019), we used SGRL in this study. Both CBR and SGRL were concentrated by nickel column chromatography purification (Fig. S4).

The actual substrates of CBR and SGR are Chl *b* and Chl *a*, respectively, which are bound to Chl-protein complexes embedded in the thylakoid membrane. Thylakoid membranes were partially solubilized by the addition of Triton X-100, a mild detergent that is commonly used for the isolation of intact LHCII. After incubation with CBR, HMChl *a* was detected using HPLC (Fig. 2). This indicates that CBR reduced Chl *b* on Chl-protein complexes. When the solubilized thylakoid membrane was incubated with a mixture of CBR and SGRL, the levels of the produced HMChl *a* increased. This indicates that the reaction of SGRL promotes the CBR reaction. Pheophytin *a* produced by the SGRL reaction may be released from the Chl-protein complex, resulting in the loosening of the structure of the Chl-protein complex. A loosened structure may enable CBR to efficiently access its substrate. The same assay was performed using SGRL instead of CBR. When the solubilized thylakoid membrane was incubated with SGRL, pheophytin *a* was detected. When the solubilized thylakoid membrane was incubated with a mixture of SGRL and CBR, the level of pheophytin *a* was increased. This suggests that the reaction of CBR enhances the reaction of SGRL. Chls bound to loosened-structure Chl-protein complexes are supposed to be catabolized in a mixture of SGRL and CBR. We do not exclude the possibility that free Chls dissociated from the loosened Chl-protein complexes are catabolized by CBR or SGRL. When isolated LHCII was incubated with NOL, not only HMChl *a*, but also Chl *a* were found as free pigments in green native gel electrophoresis (Horie et al., 2009). This suggests that when one of the Chls is removed by the action of the catabolic enzyme, the association equilibrium of Chl will be shifted towards the dissociated state. In whichever case, functional cooperation of SGR and CBR can be achieved. In summary, our observations suggest that Chls in Chl-protein complexes are catabolized by coordinated reactions between CBR and SGRL. Artificial liposomes with inserted LHCII are potential tools to further address the cooperative action of chlorophyll-degrading enzymes. Such an experiment remains to be conducted in the future.

Conclusions

We found that Chl catabolic enzymes were enriched in the grana margin fraction, suggesting their functional interaction in Chl breakdown. We examined this idea and found

that CBR and SGRL, which catalyze the committed step in Chl *b* and Chl *a* breakdown, cooperatively catabolized the Chls bound to Chl–protein complexes. These observations suggest that Chl catabolic enzymes co-localize in the grana margin and efficiently catabolize Chl. This study highlights the importance of enzyme co-localization and cooperation. While SGR localization was not determined in this study, SGR might accumulate in the grana margin. This remains to be proven in future studies.

Funding

This work was supported by the Japan Society for the Promotion of Science, KAKENHI [19K06700 to A.T., 16H06554 and 20H03017 to R.T., and 17K07430 to H.I.].

Figure legends

Fig. 1 Thylakoid fractionation and immunoblotting of chlorophyll (Chl) catabolic enzymes

Thylakoid membrane fractionation was examined by immunoblotting the proteins related to PSI, PSII, and Chl catabolism. Th, thylakoid membrane; GC, grana core; GM, grana margin; SL, stroma lamella.

Fig. 2 Enzymatic assay using Chl *b* reductase (CBR) and Stay-Green-like (SGRL) with the solubilized thylakoid membrane

Purified CBR and SGRL were incubated with solubilized thylakoid membrane. HMChl *a* (upper) and pheophytin *a* (lower) are the products of the CBR and SGRL reactions. These were quantified using HPLC. Error bars represent standard deviation ($n = 3$). * $p < 0.05$, unpaired *t*-test. n.d., not detected.

References

- Chen, Y., Yamori, W., Tanaka, A., Tanaka, R., Ito, H., 2021. Degradation of the photosystem II core complex is independent of chlorophyll degradation mediated by Stay-Green Mg²⁺ dechelataase in Arabidopsis. *Plant Sci.*, 110902.
- Danielsson, R., Suorsa, M., Paakkarinen, V., Albertsson, P.-Å., Styring, S., Aro, E.-M., Mamedov, F., 2006. Dimeric and Monomeric Organization of Photosystem II: DISTRIBUTION OF FIVE DISTINCT COMPLEXES IN THE DIFFERENT DOMAINS OF THE THYLAKOID MEMBRANE. *J. Biol. Chem.* 281(20), 14241-14249.
- Horie, Y., Ito, H., Kusaba, M., Tanaka, R., Tanaka, A., 2009. Participation of chlorophyll *b* reductase in the initial step of the degradation of light-harvesting chlorophyll *a/b*-protein complexes in Arabidopsis. *J. Biol. Chem.* 284(26), 17449-17456.
- Koochak, H., Puthiyaveetil, S., Mullendore, D.L., Li, M., Kirchhoff, H., 2019. The structural and functional domains of plant thylakoid membranes. *Plant J.* 97(3), 412-429.

Kuai, B., Chen, J., Hörtensteiner, S., 2018. The biochemistry and molecular biology of chlorophyll breakdown. *J. Exp. Bot.* 69(4), 751-767.

Kusaba, M., Ito, H., Morita, R., Iida, S., Sato, Y., Fujimoto, M., Kawasaki, S., Tanaka, R., Hirochika, H., Nishimura, M., Tanaka, A., 2007. Rice NON-YELLOW COLORING1 is involved in light-harvesting complex II and grana degradation during leaf senescence. *Plant Cell* 19(4), 1362-1375.

Meguro, M., Ito, H., Takabayashi, A., Tanaka, R., Tanaka, A., 2011. Identification of the 7-hydroxymethyl chlorophyll a reductase of the chlorophyll cycle in Arabidopsis. *Plant Cell* 23(9), 3442-3453.

Nishioka, K., Kato, Y., Ozawa, S.-i., Takahashi, Y., Sakamoto, W., 2021. Phos-tag-based approach to study protein phosphorylation in the thylakoid membrane. *Photosynth. Res.* 147(1), 107-124.

Obata, D., Takabayashi, A., Tanaka, R., Tanaka, A., Ito, H., 2019. Horizontal Transfer of Promiscuous Activity from Nonphotosynthetic Bacteria Contributed to Evolution of Chlorophyll Degradation Pathway. *Mol. Biol. Evol.* 36(12), 2830-2841.

Pruzinska, A., Tanner, G., Anders, I., Roca, M., Hörtensteiner, S., 2003. Chlorophyll breakdown: pheophorbide a oxygenase is a Rieske-type iron-sulfur protein, encoded by the accelerated cell death 1 gene. *Proc. Natl. Acad. Sci. U. S. A.* 100(25), 15259-15264.

Puthiyaveetil, S., Tsabari, O., Lowry, T., Lenhert, S., Lewis, R.R., Reich, Z., Kirchhoff, H., 2014. Compartmentalization of the protein repair machinery in photosynthetic membranes. *Proc. Natl. Acad. Sci. U. S. A.* 111(44), 15839–15844.

Ren, G., An, K., Liao, Y., Zhou, X., Cao, Y., Zhao, H., Ge, X., Kuai, B., 2007. Identification of a Novel Chloroplast Protein AtNYE1 Regulating Chlorophyll Degradation during Leaf Senescence in Arabidopsis. *Plant Physiol.* 144(3), 1429-1441.

Schägger, H., 2006. Tricine–SDS-PAGE. *Nat Protoc* 1, 16.

Schelbert, S., Aubry, S., Burla, B., Agne, B., Kessler, F., Krupinska, K., Hörtensteiner, S., 2009. Pheophytin pheophorbide hydrolase (pheophytinase) is involved in chlorophyll breakdown during leaf senescence in Arabidopsis. *Plant Cell* 21(3), 767-785.

Shimoda, Y., Ito, H., Tanaka, A., 2016. Arabidopsis STAY-GREEN, Mendel's green cotyledon gene, encodes magnesium-dechelate. *Plant Cell* 28, 2147-2160.

Studier, F.W., 2005. Protein production by auto-induction in high density shaking cultures. *Protein Expr. Purif.* 41(1), 207-234.

Tanaka, A., Yamamoto, Y., Tsuji, H., 1991. Formation of chlorophyll-protein complexes during greening 2. Redistribution of chlorophyll among apoproteins. *Plant Cell Physiol.* 32, 195-204.

Wang, L., Kim, C., Xu, X., Piskurewicz, U., Dogra, V., Singh, S., Mahler, H., Apel, K., 2016. Singlet oxygen- and EXECUTER1-mediated signaling is initiated in grana margins and depends on the protease FtsH2. *Proc. Natl. Acad. Sci. U. S. A.* 113(26), E3792-E3800.

Table 1. Chl contents in the fractionated thylakoid membrane.

		Chl (µg)	Chl <i>a/b</i>	Chl (%)
WT 0 dD	Thylakoid membrane	600.0	3.7	100.0
	Grana core	224.9	3.0	37.5
	Grana margin	47.9	6.0	8.0
	Stroma lamellar	39.4	5.4	6.6
<i>sgr</i> 0 dD	Thylakoid membrane	600.0	3.1	100.0
	Grana core	206.2	2.9	34.4
	Grana margin	30.5	5.6	5.1
	Stroma lamellar	28.1	6.0	4.7
<i>sgr</i> 7 dD	Thylakoid membrane	600.0	3.4	100.0
	Grana core	285.6	3.2	47.6
	Grana margin	32.2	6.7	5.4
	Stroma lamellar	19.3	7.8	3.2

Fig. 1

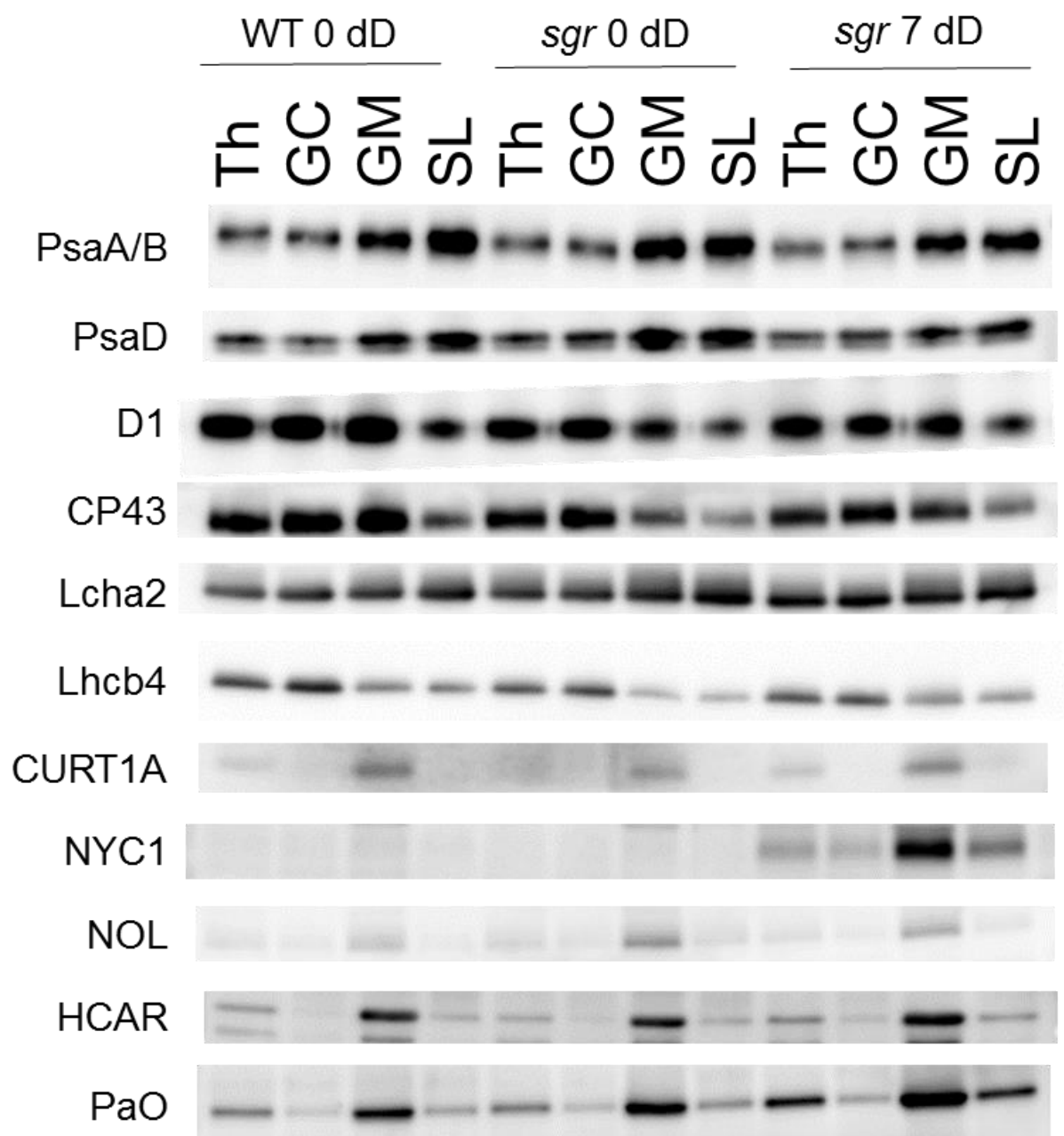
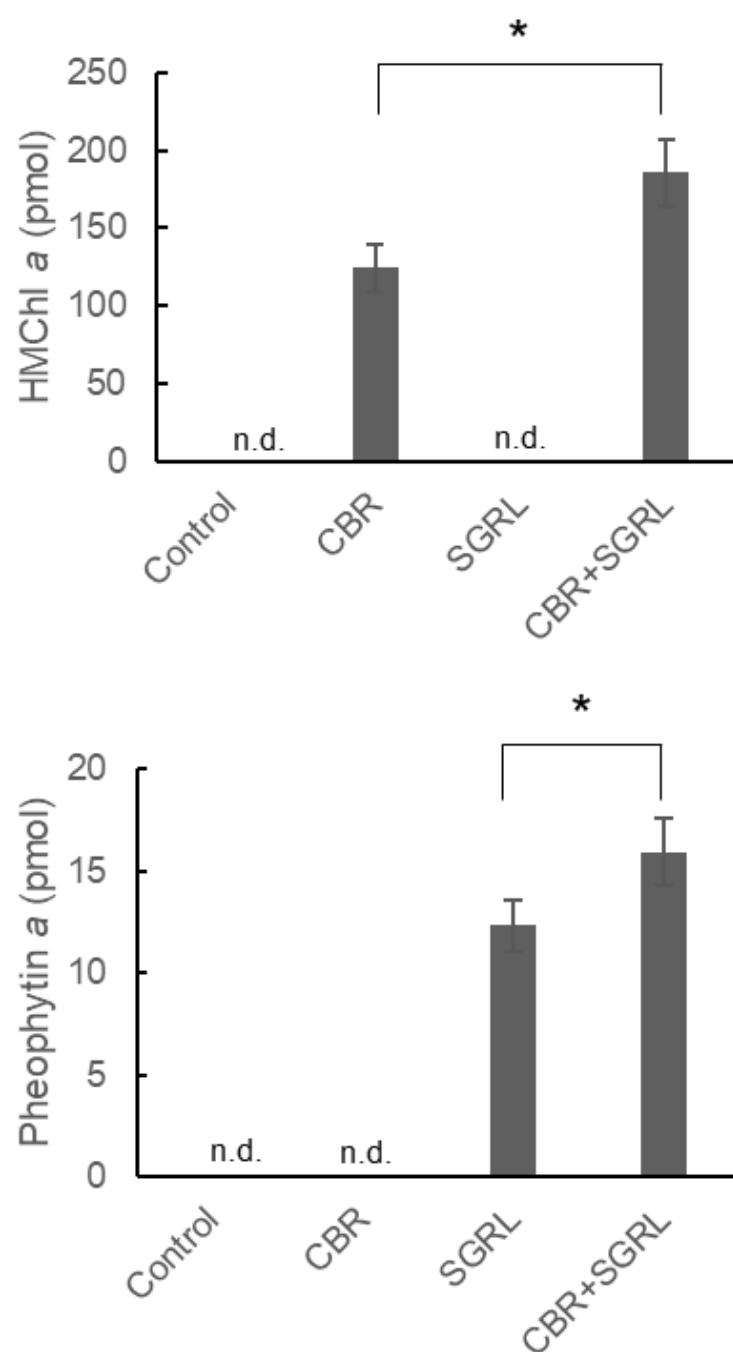


Fig. 2



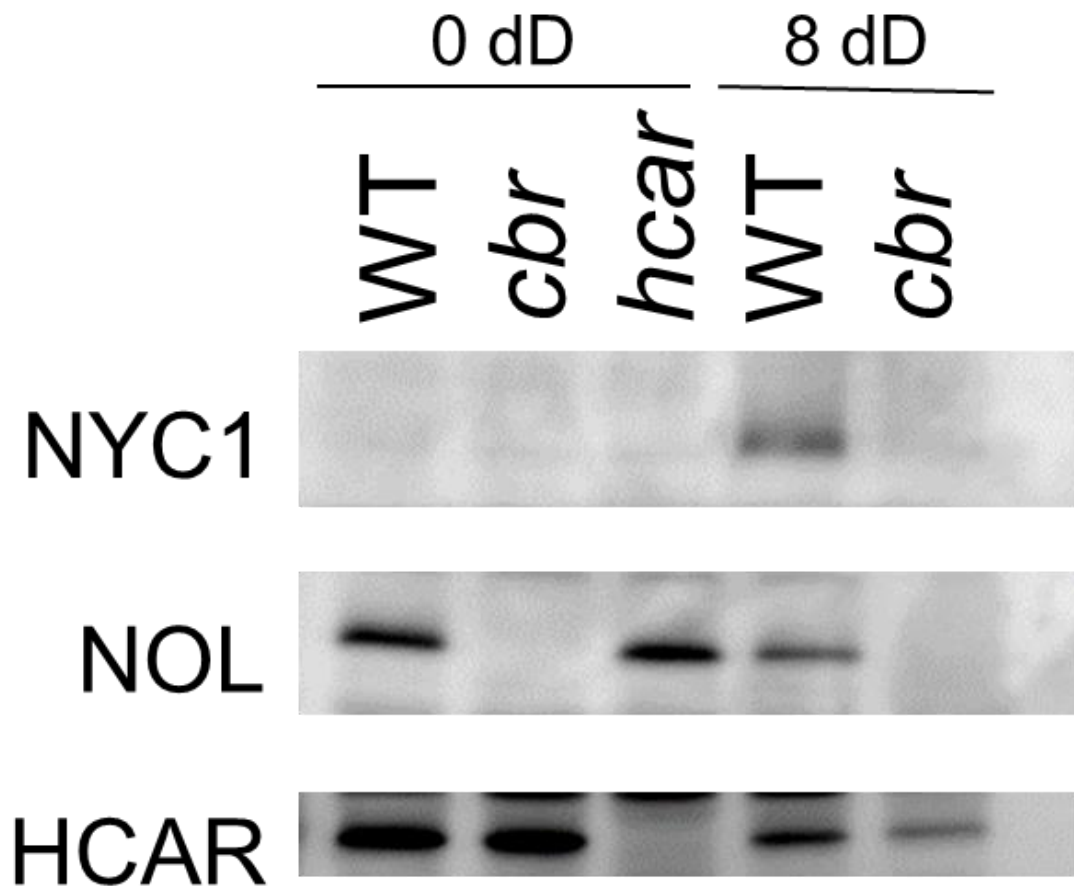


Fig. S1 Verification of the antibody specificity

NYC1, NOL, and HCAR antibodies were incubated with proteins extracted from WT, CBR-deficient, and HCAR-deficient plants. Eight-day dark-induced senescent plants were also used because NYC1 is expressed in senescent leaves.

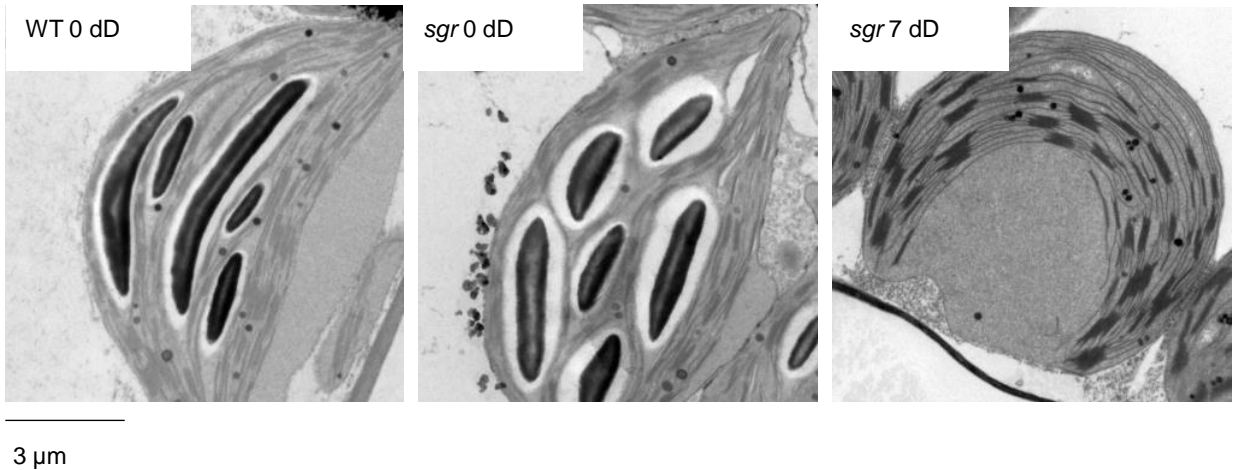


Fig. S2 Transmission electron microscopy of WT and SGR-deficient plant chloroplasts

Plants were grown for 4 weeks under 12 h light/12 h dark conditions. SGR-deficient plants were placed under dark conditions for 7 days to induce senescence. Chloroplasts were observed under a transmission electron microscope.

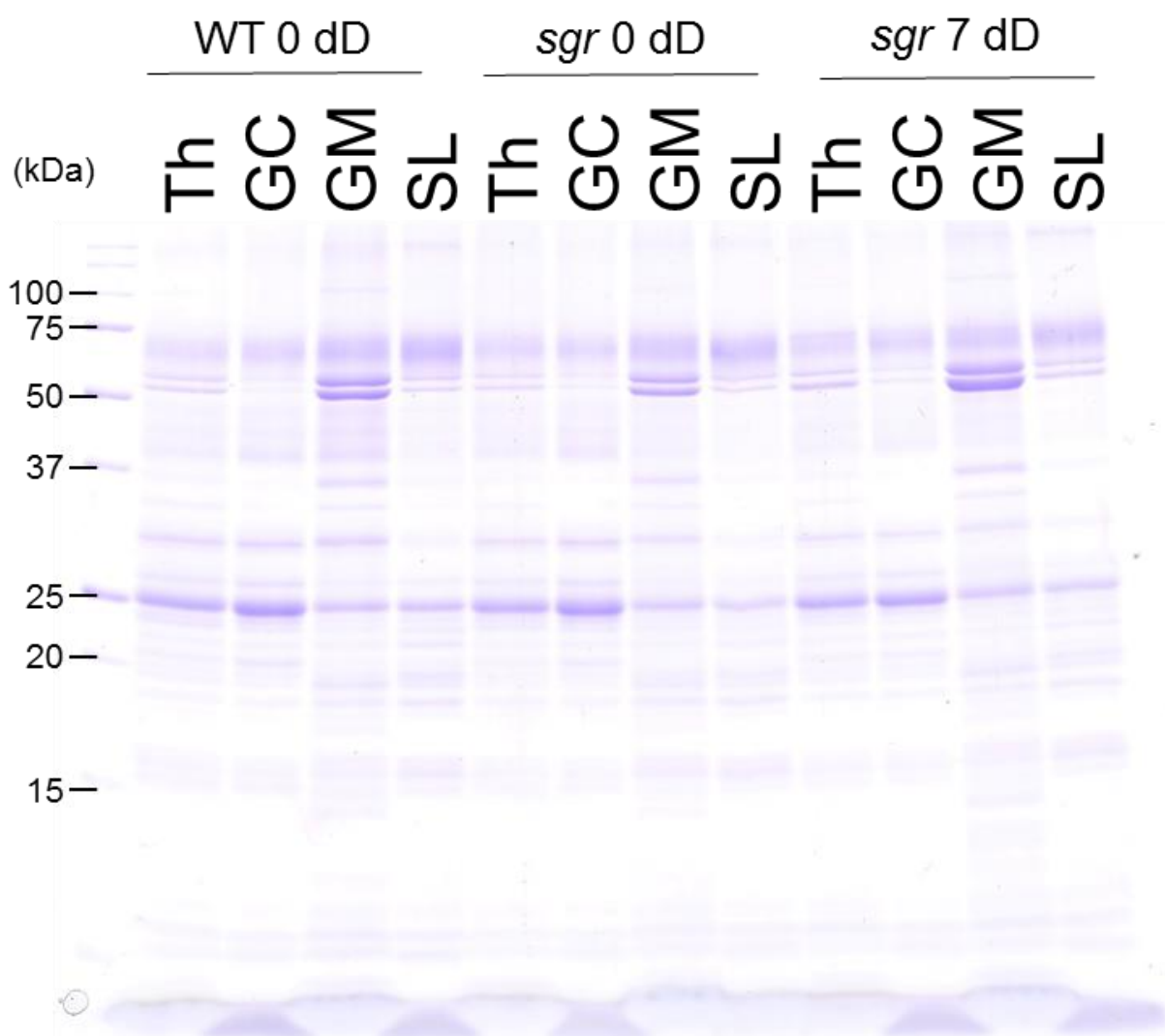


Fig. S3 Protein profiles of fractionated membranes

Isolated thylakoid membranes and fractionated membranes were applied to the gel, and proteins separated by SDS-PAGE were visualized by Coomassie brilliant blue (CBB) staining. Th, thylakoid membrane; GC, grana core; GM, grana margin; SL, stroma lamella.

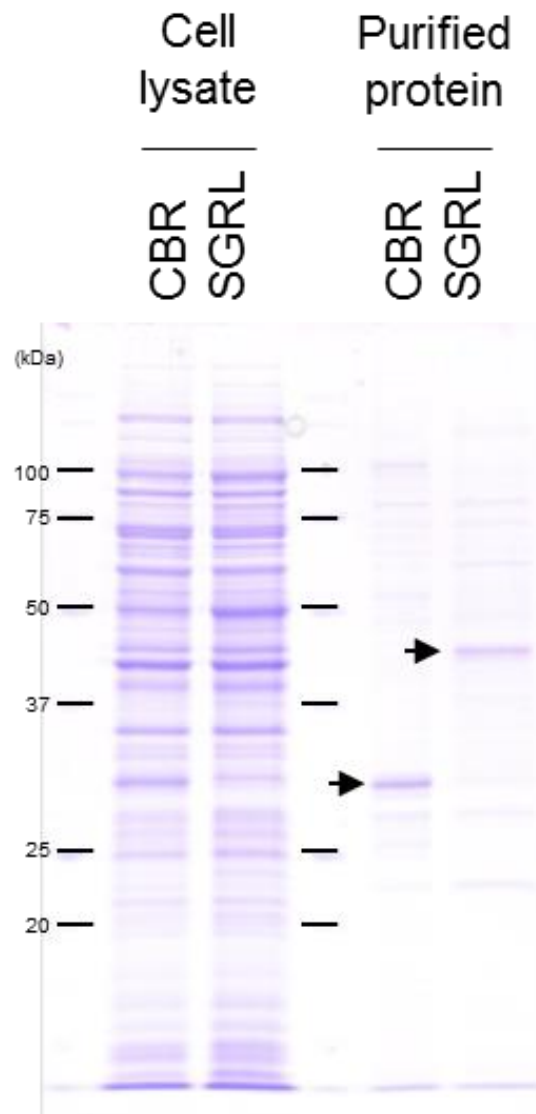


Fig. S4 Purification of the CBR and SGRL recombinant proteins

CBR and SGRL were expressed in *Escherichia coli*. The cell lysate and the nickel column-purified proteins were separated by SDS-PAGE and stained with CBB. Arrows indicate the target proteins.